Journal of King Saud University – Engineering Sciences 34 (2022) 290–301

Contents lists available at ScienceDirect

Journal of King Saud University – Engineering Sciences

journal homepage: www.sciencedirect.com

Original article

Synergistic application of polypropylene and silica nanoparticle modified by (3-Aminopropyl) triethoxysilane for cuttings transport

Jeffrey O. Oseh [a,b,d,*], M. N. A. M Norddin [a,b,c,*], Issham Ismail [a,b], Augustine Agi [a,b], Afeez O. Gbadamosi [a,b,d], Abdul R. Ismail [a,b], Prasad Manoger [a,b], Kumaresan Ravichandran [a,b]

[a] Department of Petroleum Engineering, School of Chemical and Energy Engineering, Universiti Teknologi Malaysia, 81310 Johor Bahru, Malaysia
[b] Malaysian Petroleum Resources Corporation Institute for Oil and Gas (MPRC-UTM), Universiti Teknologi Malaysia, 81310 Johor Bahru, Malaysia
[c] Advanced Membrane Technology Research Center (AMTEC), Universiti Teknologi Malaysia, 81310 Johor Bahru, Malaysia
[d] Department of Chemical and Petroleum Engineering, College of Engineering, Afe Babalola University, Ado-Ekiti, P.M.B. 5454, Ekiti State, Nigeria

ARTICLE INFO

Article history:
Received 13 March 2020
Accepted 18 October 2020
Available online 24 October 2020

Keywords:
Annular velocity
(3-Aminopropyl) triethoxysilane
Cuttings sizes
Cuttings transport
PP-SiO_2 NC-NH_2
Rheological properties

ABSTRACT

Achieving the desired efficiency in cuttings transport has always been a challenge during drilling situations due to complex wellbore trajectories and drilling hydraulics. These issues require suitable additives to formulate the drilling muds. Hence, nanocomposite (NC) particles formed from silica and polypropylene was modified by (3-Aminopropyl) triethoxysilane (termed PP-SiO_2 NC-NH_2) and the impact of the concentrations of the PP-SiO_2 NC-NH_2 between 0.4 and 1.2 ppb on the cuttings transport efficiency (CTE) of complex water-based mud (WBM) system was assessed. Mud system containing 0.5 ppb PP-SiO_2 NC-NH_2 on CTE was measured and compared with that of partially hydrolyzed polyacrylamide (PHPA) using sandstone grains of diameters between 0.50 and 3.20 mm at hole angles 0, 30, 45, 60, and 90° with a 42 L/min pump rate. The zeta potential (ζ-potential), particle size distribution, morphology, and temperature resistance of the NC were examined. The ζ-potential data revealed the stability and the long-term stabilization of the modified NC in drilling muds. By adding the concentration of the modified NC into the WBM system, the thinning characteristics and consistency factors were enhanced as the NC concentration increases. Furthermore, the rheological test program reveals that the NC concentrations and 0.5 ppb PHPA increased the shear stress of the WBM with an increase in the shear rate. However, the mud system of PHPA exhibited a larger viscosity, while the NC samples showed a flat viscosity-profile. Also, the NC demonstrated better cuttings recovery than the PHPA product at 0.5 ppb concentration, especially at the worst hole angle of 45°. The cuttings recovery from a minimum to a maximum was found to occur in this order; 45°, 60°, 30°, 90°, and 0°. In contrast with the smallest and intermediate sand grains, the largest grains have complex and less fluid transport. With a pipe orbital motion of 150 rpm and a pump rate of 42 L/min, the CTE of the muds showed higher improvement. Overall, the mud properties of the modified NC exhibited a strong enhancing impact on the cuttings carrying capacity of the base mud than the PHPA.

1. Introduction

In drilling operations, the most important task of drilling mud is to lift cuttings from the annulus when there is circulation and keep the cuttings suspended in no flow condition (Boyou et al., 2019). Poor cuttings transport is one of the major problems affecting drilling operations. This problem is often related to increased downtime and drilling cost. To assure safe and effective drilling, the drilling operator needs to make informed choices of fluid suitable for every individual well (Dahab and Al-blehed, 1992; Elkatatny et al., 2018). According to a study conducted by Bilgesu et al. (2007), annular mud velocity, pump rate, mud viscosity, hole angle,

* Corresponding authors at: Department of Petroleum Engineering, School of Chemical and Energy Engineering, Universiti Teknologi Malaysia, 81310 Johor Bahru, Malaysia.
E-mail addresses: jeffreyonuomaoseh@graduate.utm.my (J.O. Oseh), anam@utm.my (M. N. A. M Norddin).

Peer review under responsibility of King Saud University.

Production and hosting by Elsevier

https://doi.org/10.1016/j.jksues.2020.10.007
1018-3639/

Nomenclature

0.4 ppb NC	WBM + 0.4 ppb modified NC
0.5 ppb NC	WBM + 0.5 ppb modified NC
0.5 ppb PHPA	WBM + 0.5 ppb PHPA
0.8 ppb NC	WBM + 0.8 ppb modified NC
1.2 ppb NC	WBM + 1.2 ppb modified NC
API	American petroleum institute
APTES	(3-Aminopropyl) triethoxysilane
BM	Base mud
CTE	Cuttings transport efficiency
ECD	Equivalent circulating density
EtOH	Ethanol
FCT	Filter cake thickness
FESEM	Field emission scanning electron microscopy
FL	Filtrate loss volume
HTHP	High-temperature and high-pressure
K	Fluid consistency factor
n	Flow behaviour index
NaOH	Sodium hydroxides
NC	Nanocomposite
NCs	Nanocomposites
$-NH_2$	Amino groups
NH_4OH	Ammonium hydroxide
NPs	Nanoparticles
PAC HV	High viscosity polyanionic cellulose
PE–b–PEG	Polyethylene–block poly (ethylene glycol)
PP	Polypropylene
PP-SiO_2 NC	Polypropylene–silica nanocomposite
PP-SiO_2 NC-NH_2	Modified polypropylene-nanosilica composite by APTES
PSD	Particle size distribution
ROP	Penetration rate
SiO_2 NP	Nanosilica/silica nanoparticle
TEOS	Tetraethyl orthosilicate
TGA	Thermal gravimetric analysis
WBM	Water-based mud
γ	Shear rate
ζ-potential	Zeta potential
θ_3	Reading at 3 rpm
θ_{300}	Reading at 300 rpm
τ	Shear stress

pipe rotation speed, and cuttings diameters are among the significant variables that impact the cuttings transport process. An optimal annular velocity and appropriate ranges of rheological properties are often desired while drilling. The reduction of the annular velocity close to the wall hampers cuttings transport in high hole angle wells (Ozbayoglu and Sorgun, 2010). Pipe orbital rotation is desirable for cuttings transport due to its ability to expose cuttings to a higher mud velocity by mechanical action (Boyou et al., 2019). Different cuttings diameters dictate the flow pattern of the flowing mud stream with drilled cuttings (Elochukwu et al., 2017). All these mentioned variables depend on one another in the cuttings transport program and it is, therefore, necessary to study their influence on the cuttings recovery efficiency.

With the growing environmental concern, the petroleum industry now lays greater emphasis on the use of conventional water-based muds (WBMs) to drill hydrocarbon wells. Partially hydrolyzed polyacrylamide (PHPA) is widely used in the field due to its efficient viscosifying-effect in WBMs, which normally improved the properties and functions of the muds (Lam et al., 2015). Nevertheless, under the bottom-hole environments, its viscosity can become extreme, making water to separate from the mud. This factor has hampered the cuttings lifting efficiency of PHPA mud system (Ercan and Ozbayoglu, 2009). Using the benefit of polymeric and nanoscale agent to design a well-dispersed and less-viscous drilling fluid could help to enhance the poor heat resistance of PHPA-WBM under the bottom-hole environments.

Today, the hybrid of polypropylene (PP) and silica nanoparticle (SiO_2 NP) or nanosilica to form polymer nanocomposite has been extensively studied in different fields (Zu et al., 2013; Mao et al., 2015). PP possesses strong viscoelastic properties, self-assembly, efficient heat, and chemical resistance (Zu et al., 2013). PP molecules can easily pack and arrange themselves into tunable features, mono-layer thick surfaces with structures that can be manipulated easily for specific functionalities (Katende et al., 2020). As a result, PP is applicable in different composite blends and is effective in drilling operations. For SiO_2 NP, its attention has increased in the petroleum industry in different applications (Medhi et al., 2020). It is sought for where thermal stability, improvement in cuttings lifting, and reduction in filtrate loss are of interest (Boyou et al., 2019). Now, researchers have discovered that the performance of SiO_2-based composite will increase if the particle agglomerates are reduced by the method of surface charge modification through the attachment of surfactants, especially dispersants (Elochukwu et al., 2017; Medhi et al., 2020).

Among the various silane molecules for the surface modification of nanosilica, (3-Aminopropyl) triethoxysilane (APTES) is broadly used. This is due to the ability of the amino-functionality ($-NH_2$) to improve the dispersion and physical stability of SiO_2 fluid or suspension (Qiao et al., 2015). APTES also acts as a connection unit to attach other functional polymers or molecules to SiO_2 NP surface (Omurlu et al., 2016). The attachment of APTES to the negative surface of nanosilica-based composite was seen as a promising solution to address the SiO_2 NP agglomerates in a fluid system (Qiao et al., 2015). The presence of $-NH_2$ makes APTES so efficient for surface interactions. Therefore, attachment of APTES on the studied nanocomposite (NC) bearing the negative silanol-hydroxyl group (Si-O–H) was seen as a key to achieving efficient dispersion and long term stability of the drilling mud with higher properties' performance. This is because modified-dispersed particle offers an increased colloidal interaction with WBM additives (Zu et al., 2013). A comparison between modified and unmodified SiO_2 NP on bentonite-based drilling mud was made by Elochukwu et al. (2017). The results revealed that the mud samples of the modified SiO_2 NP have better rheological and filtration properties than the unmodified SiO_2 particle due to its stronger dispersibility and physical stability resulting from its surface modification.

In the data collected from open literature, APTES composited SiO_2 NP and PP (PP-SiO_2 NC-NH_2) has not been examined to a reasonable extent for the enhancement of the properties of complex WBM system. Further, these data do not account for cuttings transport under different types and sizes of sand grains (granite, sandstone, limestone, and dolomite). For this reason, this study examined the synergistic effect between synthetic PP and SiO_2 NP modified by APTES on the WBM system for cuttings transport. The rheological characterization of the mud systems was executed through the rheological models, Bingham plastic and Power-law basic equations.

2. Experimental

2.1. Materials

The chemicals used to synthesize and modify the PP-SiO_2 NC-NH_2 are as follows: PP (melt index of 12.3 g per 10 min), ammonium hydroxide (NH_4OH), xylene, tetraethyl orthosilicate (TEOS), polyethylene-b-poly (ethylene glycol) (PE-b-PEG) of weight ratio 50:50 (PE: PEG), APTES, and ethanol (EtOH). The materials for the drilling muds are caustic soda (NaOH), bentonite, soda ash (Na_2CO_3), barite, polyanionic cellulose of high viscosity (PAC HV), xanthan gum (XG), and PHPA. These chemicals were acquired from Sigma-Aldrich (M) Sdn. Bhd., Selangor, Malaysia and applied as acquired.

2.2. Methods

2.2.1. Synthesis of the nanocomposite

The synthesis and formation of the NC was carried out based on a previous report by Zu et al. (2013) with some changes in input variables (Fig. 1).

The synthesis involves two phases, which are hydrophobic and hydrophilic. For the hydrophobic phase, synthetic PP of 6 g was mixed with the co-polymer PE-b-PEG of 24 g at 160 °C and a torque-speed of 300 rpm in a Plasti-Corder Brabender. Xylene of 20 ml was used to dissolve the mixture and the dissolved mixture was stirred at 140 °C and 300 rpm for 2 h with a magnetic agitator. TEOS of 20 ml was introduced into the sample gently and the mixing was continued for 10 min. Then, the sample was introduced gently into the hydrophilic solution prepared by mixing 60 ml of NH_4OH and 100 ml of EtOH. The stirring of the sample continued for an extra 30 min at 80 °C. It was cooled for 24 h at 25 °C. The method of centrifugation for 40 min at 6000 rpm was applied to recover the product in solid form. The product was washed with EtOH to eliminate contaminants and oven-dried for 24 h at 60 °C. The dried product was denoted as synthesized PP–SiO_2 NC.

2.2.2. Zeta potential investigation of acquired TEOS

Before the synthesis, the ζ-potential of the SiO_2 precursor, TEOS was measured by dispersing 0.001 ml of the TEOS in 100 ml deionized water. Malvern Nano ZSP (Malvern Instruments Inc. Westborough MA, USA) was employed to examine the ζ-potential of the acquired TEOS. The obtained result indicated that the TEOS has a ζ-potential number of −0.4 mV, as shown in Fig. 2, which indicates instability that can result in particle aggregation.

2.2.3. Surface modification and zeta potential of PP–SiO_2 NC

For surface modification of the synthesized NC, four different concentrations of the NC between 0.4 and 1.2 ppb were introduced into a prepared solution of 40 ml EtOH/100 ml deionized water. The mixture was homogenized for 10 min at 25 °C with Silverson Homogenizer. Then, a constant amount of APTES (1.4 ml) was introduced dropwise into the solution and mixed for another 10 min. After the stirring, ultrasonication energy was employed to further disperse the mixture at 60 °C for 10 min, while the pH was changed with 0.50 M NaOH to 8.0 for all the concentrations. Thereafter, the mixture was placed in a centrifugation machine at a torque-speed of 4000 rpm for 40 min and the supernatant was decanted. The precipitates were washed with EtOH to eliminate any contaminants. They were freeze-dried and branded PP-SiO_2 NC–NH_2 (modified NC). Fig. 3 illustrates the process used to graft positive amine molecules onto the negative surface charge of the synthesized NC.

2.2.4. Characterization of PP-SiO_2 NC and PP-SiO_2 NC-NH_2

To expound the changes in the morphologies and molecular structures of the PP-SiO_2 NC-NH_2 and PP-SiO_2 NC, the Field Emission Scanning Electron Microscopy (FESEM) (Ultra, Zeiss, Germany) with a high magnification of 6.0 KX was used. The temperature resistance of the NCs was measured using Thermal Gravimetric Analysis (TGA) by scanning 0.02 g of the NCs from 30 °C to 600 °C at a heating rate of 10 °C/minutes. The measurement was conducted on a TGA Build 39, Q500V20.13 (TA Instruments, Germany).

2.2.5. Formulation of drilling muds

The acronyms of the different mud samples formulated are shown in Tables 1, while 2 shows the formulation of the mud samples following the API protocols (API RP 13B-1, 2017). 9.5 ppg weighted muds were formulated based on the recommendation of previous studies (Al-Awad, 2001; Al-Awad and Al-Qasabi, 2001) where mud weight between 9.0 and 10.0 ppg was suggested as the optimal mud formulation for WBMs. The mud samples were

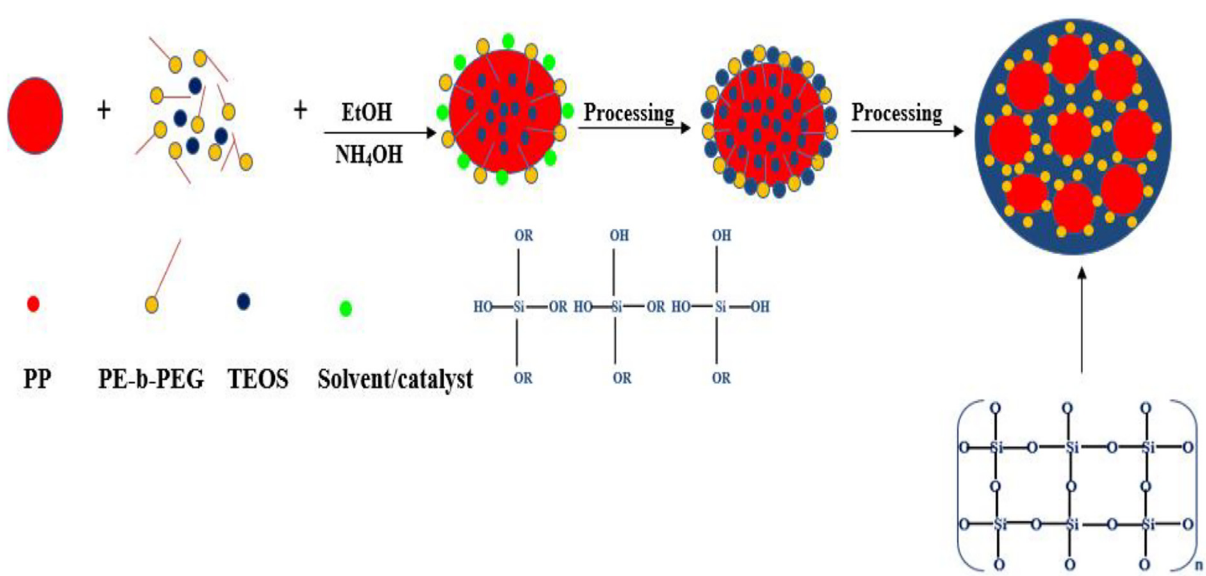

Fig. 1. Synthesis and formation of the nanocomposite.

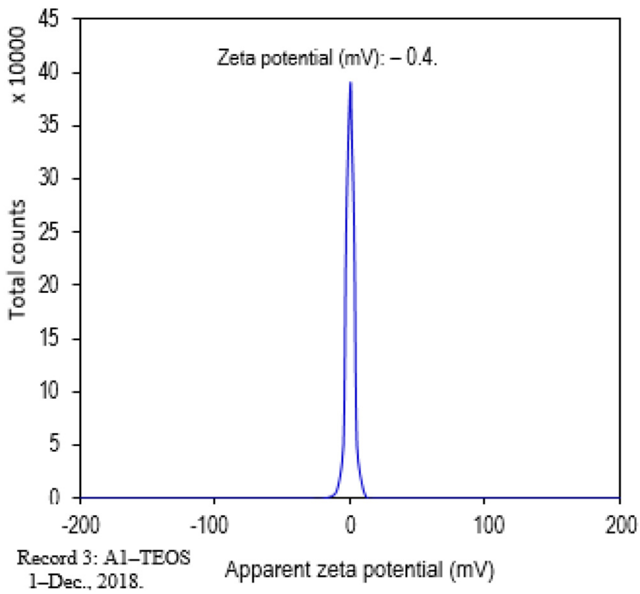

Fig. 2. Surface charge of acquired TEOS.

formulated to possess a higher YP than PV to assure higher lifting of cuttings in the cuttings lifting process.

2.2.6. Rheological characterization

The mathematical models, Bingham plastic and Power- law basic fluid characterization, which remains prevalent for description in the field (Nelson and Guillot, 2006; Sayindla et al., 2017) were applied to evaluate the viscosity-profile of the drilling muds following the API testing protocols (API RP 13B-1., 2017). The rheological test program was conducted before (25 °C) and after (150 °C) aging in a dynamic 4-roller aging cell by using a 6-speed Fann Viscometer, Model 35A (Houston, TX, USA). The values of shear stress under stabilized shear rate conditions between 5.11 and 1022 s^{-1} were registered against six different dial readings between 3 and 600 rpm. The measurements were repeated twice to establish reproducibility and the averages recorded. The Bingham plastic basic equations applied to determine the rheological behaviour of the different mud systems are presented in Eqs. (1)–(3).

Table 1
Formulated drilling muds and their acronyms.

Mud samples	Acronyms
WBM	BM
WBM + 0.4 ppb modified NC	0.4 ppb NC
WBM + 0.5 ppb modified NC	0.5 ppb NC
WBM + 0.8 ppb modified NC	0.8 ppb NC
WBM + 1.2 ppb modified NC	1.2 ppb NC
WBM + 0.5 ppb PHPA	0.5 ppb NC

Table 2
Compositions of WBMs with modified NC and PHPA.

Muds	Mud compositions in a laboratory scale
BM	320.34 ml water + 15 ppb bentonite + 0.25 g NaOH + 0.25 g Na_2CO_3 + 0.20 g XG + 2.0 g PAC HV + 34.22 g barite.
A-0.4	320.21 ml water + 15 g bentonite + 0.25 g NaOH + 0.25 g Na_2CO_3 + 0.20 g XG + 2.0 g PAC HV + 33.95 g barite + 0.4 ppb modified NC.
A-0.5	320.13 ml water + 15 g bentonite + 0.25 g NaOH + 0.25 g Na_2CO_3 + 0.20 g XG + 2.0 g PAC HV + 33.93 g barite + 0.5 ppb modified NC.
A-0.8	320.11 ml water + 15 g bentonite + 0.25 g NaOH + 0.25 g Na_2CO_3 + 0.20 g XG + 2.0 g PAC HV + 33.65 g barite + 0.8 ppb modified NC.
A-1.2	320.01 ml water + 15 g bentonite + 0.25 g NaOH + 0.25 g Na_2CO_3 + 0.20 g XG + 2.0 g PAC HV + 33.35 g barite + 1.2 ppb modified NC.
B-0.5	320.13 ml water + 15 g bentonite + 0.25 g NaOH + 0.25 g Na_2CO_3 + 0.20 g XG + 2.0 g PAC HV + 33.93 g barite + 0.5 ppb PHPA.

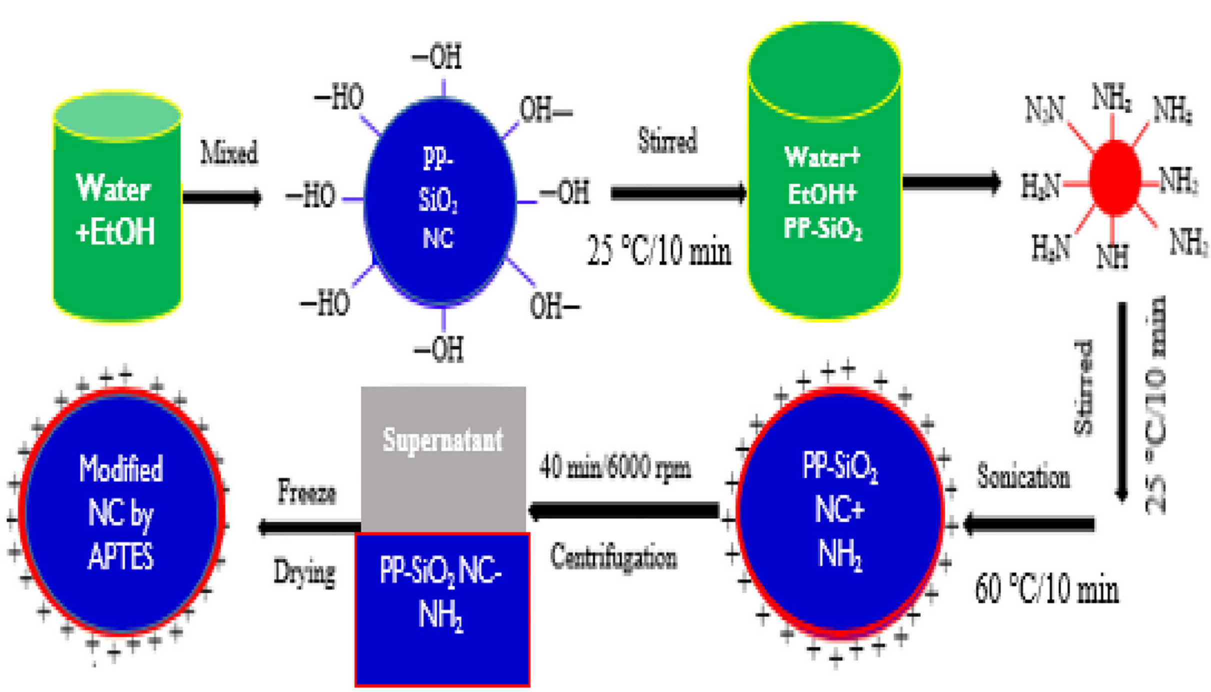

Fig. 3. Procedure used to modify the surface of the NC.

$$\text{Effective viscosity } (\mu_a = \text{Pa.s}) = \frac{300 \times \theta}{\omega} \quad (1)$$

$$\text{Shear rate } (\gamma = s - 1) = 1.7023 \times \omega \quad (2)$$

$$\text{Shear Stress } (\tau = \text{Pa}) = 1.065 \times \theta \quad (3)$$

where θ (Pa.s) is the dial reading and ω (rpm) is the rotor speed.

2.2.7. Filtration measurements

API filtrate loss or fluid loss (API FL) tests were performed in a standard API filtrate loss equipment (Fann Instrument Company, Houston, TX, USA). A 100 psi (0.69 MPa) pressure was injected through a nitrogen cylinder from the top and the muds were made to pass through a filter paper placed at the bottom of the cylinder. The measurement was made for 30 min at ambient temperature. The mud that seeps through the filter paper was then collected in a test tube and the volume of the collected mud was measured, representing the API FL. The thickness of the muds deposited in the filter paper was measured with a Vernier caliper indicating the API filter cake or mud cake thickness (API FCT). The same process was repeated to measure the high-temperature and high-pressure (HTHP) filtrate loss volume (HTHP FL). The test differential pressure and the temperature in the heating jacket was 500 psi (3.45 MPa) and 150 °C, respectively. For accurate test data, the tests were performed twice and average readings registered.

2.2.8. Preparation of sand grains

The grains of four different sand types (sandstone, granite, limestone, and dolomite) were sieved into four different diameters from 0.50 to 0.85 mm, 1.00 to 1.70 mm, 2.00 to 2.40 mm, and 2.80 to 3.20 mm following the recommended American Society for Testing and Materials protocols (ASTM, 2006). The sieved grains were washed and dried thoroughly before injecting them into the flow loop.

2.2.9. Cuttings transport experiment in a flow loop

A field-scale down cuttings transport flow loop was built purposely to investigate the efficiency of drilling muds in the cuttings transport process, as presented in Fig. 4.

The flow loop has been designed to simulate closely field conditions in vertical and low hole angles (0–30°), deviated (31–89°), and horizontal (90°) wellbores according to a previous study performed by Boyou et al. (2019). A representation of the flow loop is shown in Fig. 5.

In a laboratory test of cuttings transport efficiency carried out by Ozbayoglu and Sorgun (2010), it was stated that laboratory results generated in a 12-ft. annulus could provide reasonable precisions (within 10% from the experimental correlations). Hence, in this study, the total wellbore simulator was 10.67 m (35-ft.) long, providing enough distance for the flow to become fully stabilized. The annular area consists of an acrylic pipe of 4.88 m (16-ft.) long in an attempt to gain a higher precision of cuttings transport performance. The annular test section simulates a cased hole of 60.96 mm (2.4-in.) inner diameter and a rotatable drill pipe with an outer diameter of 30.48 mm (1.2-in.). The rotatable drill pipe was placed inside the transparent acrylic pipe to create a concentric annular environment (i.e. 0% eccentricity annulus).

The experiments were conducted using four different annular mud velocities starting from 66.1 ft/min (20.1 m/min), 92.4 ft/min (28.2 m/min), 118.8 ft/min (36.1 m^3/min), and to a maximum value of 138.6 ft/min (42.2 m/min). The annular test section was set at a constant pipe angle of 60° for the investigation of BM and BM + PP-SiO_2 NC-NH_2 using three different concentrations (0.4, 0.8, and 1.2 ppb) of the modified NC without a rotatable inner drill pipe. Thereafter, the pipe angle was varied from 0°, 30°, 45°, 60°, and 90° from the vertical to mirror a complete wellbore. For comparison between the modified NC and PHPA, only 0.5 ppb concentration with sandstone cuttings was investigated.

0.5 ppb concentration was selected because drags reducing polymer, such as PHPA is more effective at lower concentrations than at higher dosage (Ercan and Ozbayoglu, 2009). Besides, it may be difficult to pump and circulate the muds effectively with

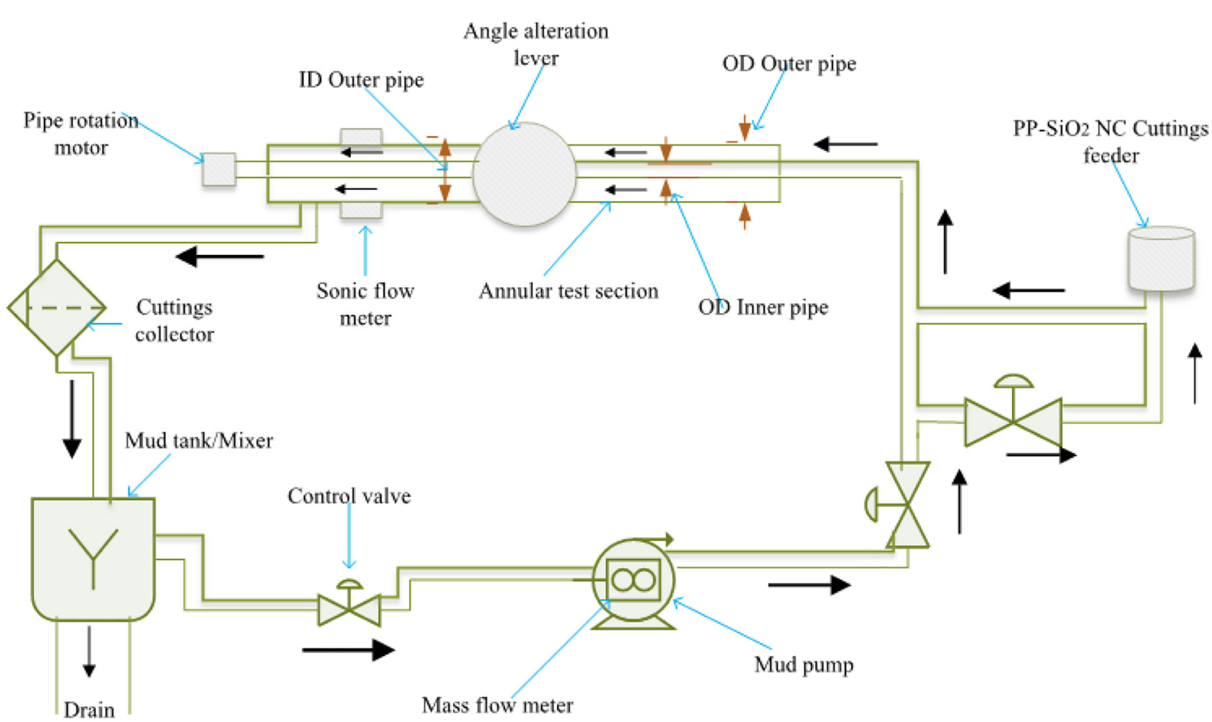

Fig. 4. Schematic of cuttings rig simulator.

Fig. 5. Layout of cuttings rig simulator.

the available pump capacity of 42 L/min (0.042 m^3/min) if the PHPA concentration was larger than 0.5 ppb. This is because long-chain PHPA molecules at high dosage can induce excessive equivalent circulation density (ECD) (Al-Awad, 2001; Ercan and Ozbayoglu, 2009). The CTE was determined both when the pipe was set to rotate at 150 rpm and when it was static. 200 g of each of the test sand was added into the cuttings rig simulator through the cuttings feeder for each test. The drilling muds were circulated using a 2-HP variable speed centrifugal pump with the capacity of 150 L mud tank. The cuttings were separated from the muds using a cuttings separator of 0.2 mm wire mesh. The lifted cuttings were recovered after seven minutes of the circulation process and five minutes of recirculation to clean out any remaining cuttings inside the circulation pipes before conducting a new experiment. The tests were performed two times and the averages recorded. The cuttings transport efficiency (CTE) was calculated by measuring the rate at which the cuttings are removed from the rig simulator to the rate at which the cuttings are initially injected into the simulator.

3. Results and discussions

3.1. PSD analysis

The PSD characterization results and the average specific surface area of the NC with and without surface modification are shown in Fig. 6. The shapes of the curves in Fig. 6a and b are similar but the modified sample (Fig. 6b) showed a wider particle distribution due to the presence of APTES molecules in the modified product (Fig. 6b) (Omurlu et al., 2016). The particle size of the unmodified predominantly ranged from 77 to 370 nm with the median size (D_{50}) of 184 nm (Fig. 6a), while that of the modified was mainly distributed between 80 and 390 nm with a D_{50} of 189 nm (Fig. 6b). The unmodified product has a mean particle size of 122 nm and a peak frequency of 232 nm (Fig. 6a), while the modified sample showed a higher mean particle size of 146 nm and a peak frequency of 252 nm (Fig. 6b).

According to Fig. 6c, the NC products have fairly enough average specific surface area (18.6 m^2/g for unmodified) and (13.7 m^2/g for modified). The lower average specific surface area of the modified NC might be due to the adsorption of APTES onto the inner surface of the NC and micropore (Mao et al., 2015). Given these results, the surface charge modification of the nanocomposite can be established.

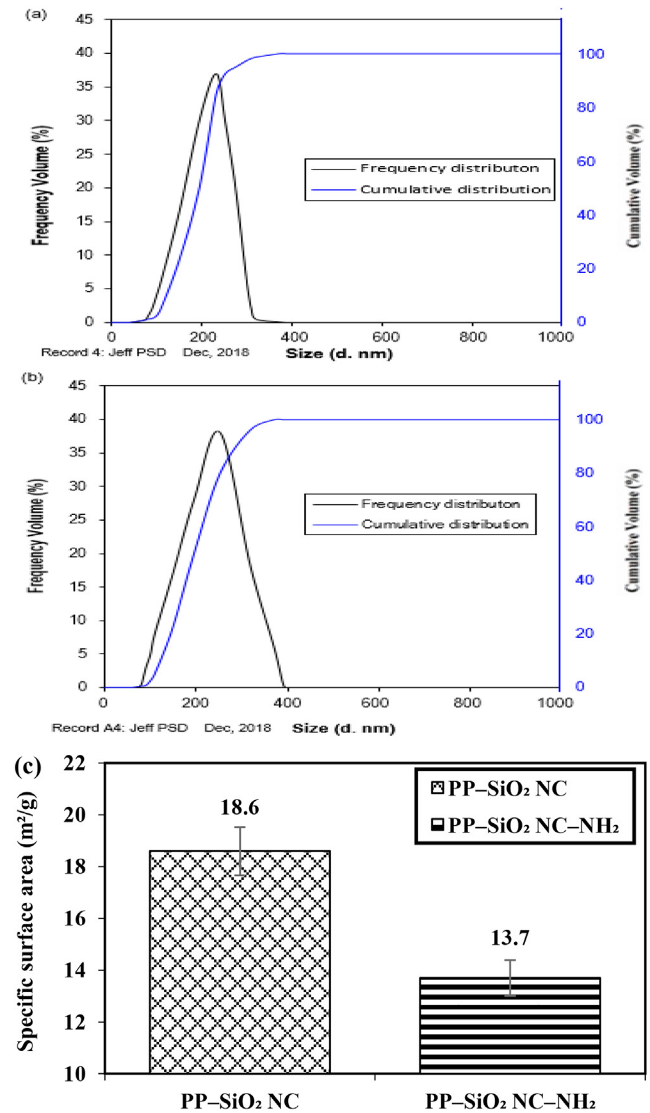

Fig. 6. PSD result of (a) Unmodified NC (b) modified NC, and (c) specific surface area of nanocomposite products.

3.2. Influence of APTES on the nanocomposite

The ζ-potential results of the modified and unmodified NC samples were determined at 25 °C (78 °F) and 150 °C (300 °F). These results are shown in Fig. 7. The unmodified product showed negative ζ-potential magnitudes before and after aging tests in the range between −7.22 mV and −6.19 mV (25 °C) and between −5.24 mV and −4.53 mV (150 °C). These values are in the region of instability and will lead to agglomeration of mud particles (Medhi et al., 2020). After modification by APTES, the samples moved to a high net positive magnitudes between +43.1 mV and +42.4 mV at 25 °C and between +40.4 mV and + 37.2 mV at 150 °C because of the amino (–NH_2) groups on the surface of the modified NC. The modified particles showed strong stability at a higher temperature of 150 °C, which indicates their long term stabilization in high-temperature environments (Oseh et al., 2020a, 2020b). Therefore, cuttings transport experiments were conducted using the modified PP-SiO_2 NC-NH_2 product. These data also supported the surface modification of the evaluated nanocomposite product.

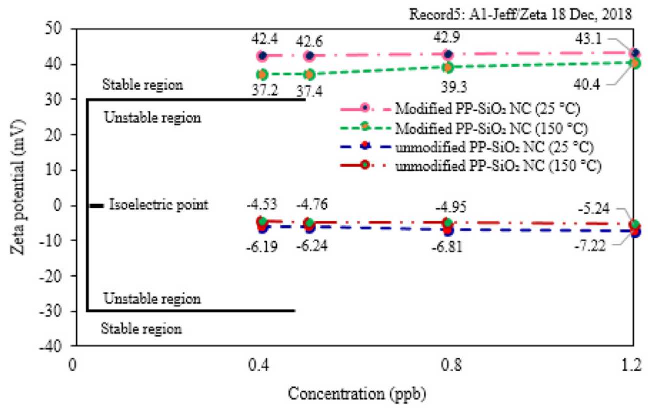

Fig. 7. The average ζ-potential of APTES modified and unmodified PP–SiO_2 NC samples.

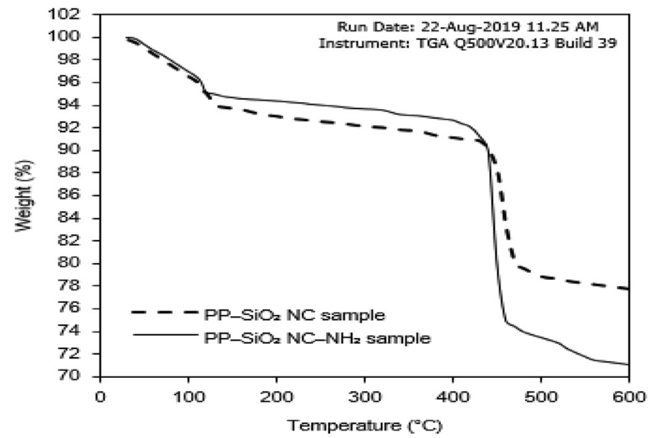

Fig. 9. Thermal stability of modified and unmodified NCs.

3.3. FESEM images of nanocomposite products

Fig. 8 depicts the FESEM images of unmodified (left) and modified (right) PP–SiO_2 NC samples. The particles were partially aggregated and stuck to each other (i.e. they formed irregular clusters or aggregates in a cotton wool-like form) Fig. 8 (left). For the amino-modified sample presented in Fig. 8 (right), the particle morphology appears spherical and regular with a less cotton wool-like form indicating that they have fine-dispersibility in dilute aqueous solution (Medhi et al. 2020; Oseh et al., 2020c). The amount of the amino groups increased the dispersibility of the PP-SiO_2 NC-NH_2 further verifying that the functionalization of the evaluated nanocomposite met the design objective.

3.4. TGA analysis of modified and unmodified PP–SiO_2 NC

The TGA curves of modified and unmodified NC are presented in Fig. 9. The shapes of their trend lines are similar. The overall weight loss of the unmodified NC occurred between 430 and 460 °C attributed to the complete breakdown of the structure of the unmodified product. For the modified product, the complete degradation of its structure occurred between 420 and 460 °C. In comparing these two products, between the temperature range of 30 and 500 °C, a total weight loss of the unmodified sample showed 21.2% and this loss was lower than that of the modified of 26.5%. This event was due to an increased number of molecules grafted onto the modified product. Nevertheless, the modified product demonstrated a strong character of temperature resistance. These data also interpret that the modification of the evaluated NC was achieved.

3.5. Rheological behaviour of drilling muds

Today, in drilling operations, the shear rate rarely surpasses 250 s^{-1} which is for the 8.5 in. section and equivalent. For a 17.5 in. section, the shear rate rarely surpasses 50 s^{-1}. Therefore, for better accuracy of fluid characterization and viscosity-profile during drilling situations, fluid characterization based on the descriptions of rheological behaviour provides an appropriate estimate of the possible pump rates needed (Oltedal et al., 2015; Elkatatny et al., 2018). Fig. 10 shows the rheological behaviour of modified NC concentrations at 25 °C (Fig. 10a) and 150 °C (Fig. 10b) under different shear rates in a log–log scale. The rheogram displayed that the shear stress of the WBM system was increased with an increase in the shear rate when the NC concentrations and 0.5 ppb PHPA were introduced. However, the mud system of PHPA

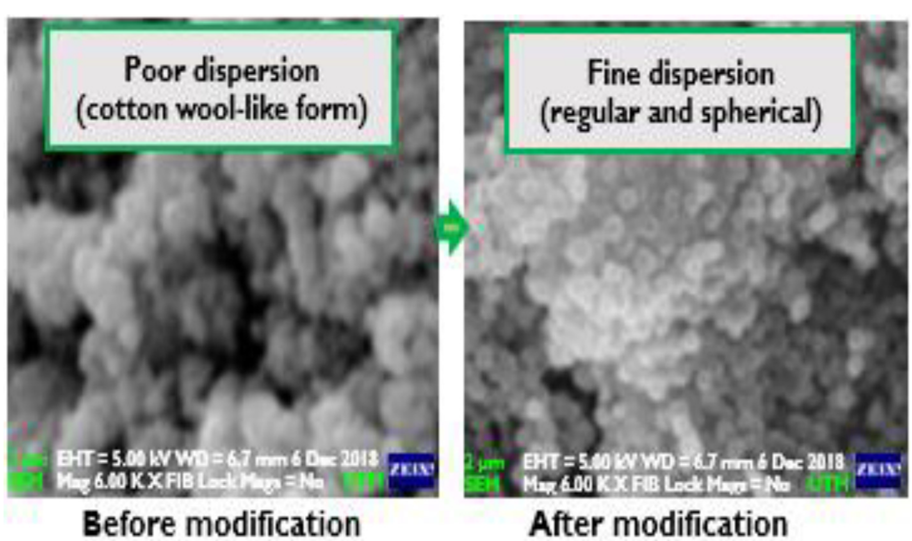

Fig. 8. FESEM images of Unmodified (left) and modified (right) PP–SiO_2 NC products.

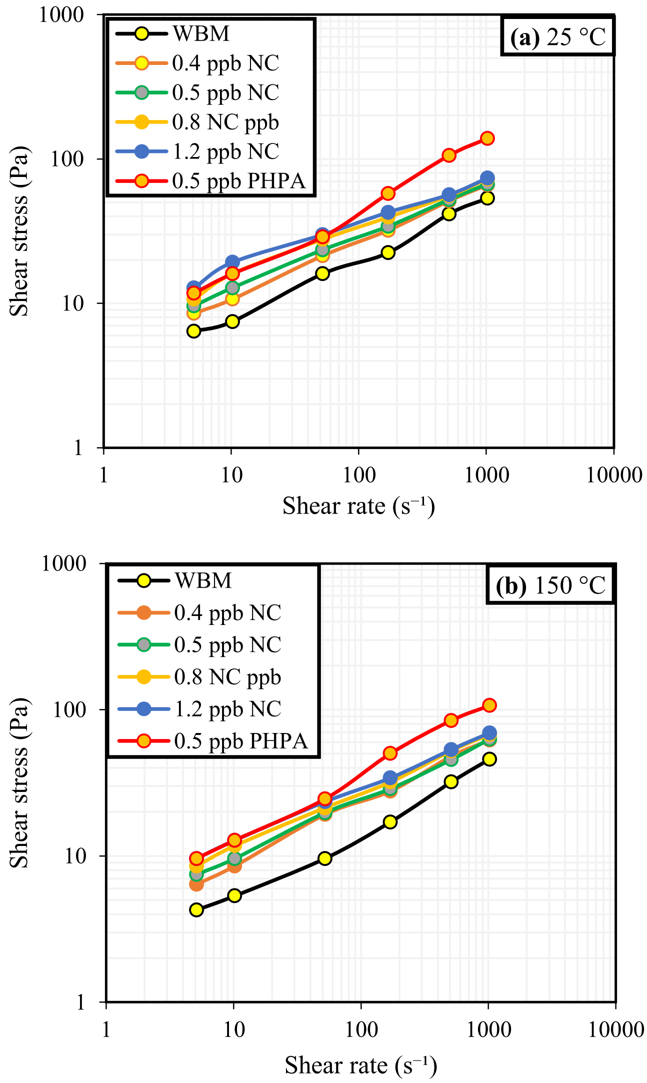

Fig. 10. Shear stress of modified NC and PHPA versus shear rate (a: T = 25 °C; b: T = 150 °C).

exhibited a larger viscosity over all the NC concentrations, while the NC samples showed a flat viscosity-profile. The hydrogen atoms present in the NC formed hydrogen bonds with water molecules. So, the strength of the intermolecular interaction between the NC and the water molecules control the PP-SiO_2 NC-NH_2 rheology (Medhi et al., 2020).

With 0.5 ppb PHPA in the mud, the shear stress increased significantly before and after aging because of the fast formation of PHPA long-chain and stability of the macro-molecular structure of the PHPA. Besides, the molecules of PHPA are a flexible chain that remains in a coil-like structure in the lack of a shearing effect. This effect led to higher entanglement of PHPA flexible chains, which is the prime element in its viscosity (Ercan and Ozbayoglu, 2009). However, under the bottom-hole condition, the PHPA mud sample at 1022 s^{-1} (trend line 0.5 ppb in red) exhibited the largest margin of reduction in the shear stress by 23.1% (from 138.71 to 106.7 Pa). With similar NC concentration (trend line 0.5 ppb in green), only 6.4% reduction in the shear stress (from 67.22 to 62.95 Pa) was observed, while the base fluid (trend line in black) reduced by 14.0% (from 53.35 to 45.89 Pa). Given these data, the modified NC has a promising fluid flow property under bottom-hole conditions than the PHPA.

Further, the viscosities under different shear rates before and after the fluid aging operation in a log–log scale are shown in Fig. 11a and b.

According to these figures, the viscosities of NC and PHPA mud systems were decreased with increasing shear rates, thus, indicating a non-Newtonian and pseudoplastic character from lowest shear rate (5.11 s^{-1}) to highest shear rate (1022 s^{-1}). It can also be observed that the 0.5 ppb PHPA mud system (trend line in red) displayed a momentous improvement in the viscosity of the WBM as against that of the NC (trend line in green) at both temperature conditions. It even exceeded that of the 1.2 ppb NC (trend line in blue) at higher shear rates before (Fig. 11a) and after (Fig. 11b) aging. At the 0.5 ppb concentration with shear rates (between 1022 and 5.11 s^{-1}), the PHPA viscosity varies between 65 and 1100 Pa.s. For the NC at the same concentration, the viscosity varies between 31.5 and 900 Pa.s and that of the WBM system lie between the range of 25 and 600 Pa.s. This interprets that the PHPA molecules exhibited stronger intermolecular forces of attraction with water molecules through hydrogen bonding than the NC (Al-Homadhi, 2009; Lam et al., 2015).

Furthermore, the viscosity-shear rate relationship was fitted using the Ostwald-de Waele viscosity model (or Power-law model)

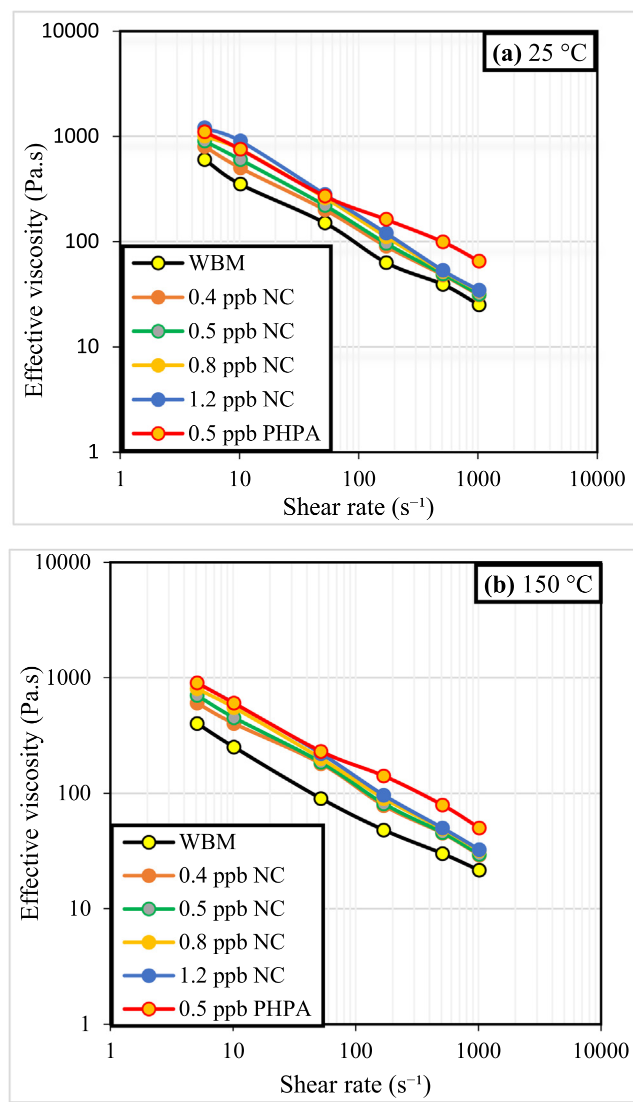

Fig. 11. Viscosity of modified NC and PHPA versus shear rate (a: T = 25 °C; b: T = 150 °C).

described by Eqs (4)–(6) and the data calculated are tabulated in Tables 3 and 4.

$$\tau = K\gamma^n \tag{4}$$

n and K factors can be determined from any two values of shear stress and shear rate.

$$n = 0.5\log\frac{\theta_{300}}{\theta_3} \tag{5}$$

$$K = \frac{5.11 \times \theta_{300}}{511^n} \tag{6}$$

where γ is the shear rate (in s^{-1}), τ is the shear stress (in Pa), θ_{300} is the reading at 300 rpm, θ_3 is the reading at 3 rpm, n is the flow behavior index (dimensionless), and K is the fluid consistency factor (in poise (P): 1P = 10 Pa).

As the NC concentration and 0.5 ppb PHPA in the base mud increases, the consistency factor (K) also displayed a corresponding increase. This typifies an enhancement in the viscosity of the base fluid for higher cuttings transport capacity. Also, the flow behaviour index (n) of the base fluid decreases with increasing NC concentration. This translates to improvement in the shear-thinning behaviour of the base fluid system with the modified NC. However, with 0.5 ppb PHPA, the flow behaviour index of the base fluid increases, indicating the possibility of larger viscosity of PHPA at higher concentrations, which can make the mud system inefficient under bottom-hole conditions. From the rheological characterization, the modified NC is seen as positive for improvement in the cuttings transport jobs and drilling program.

3.6. Filtration characterization of mud samples

Other mud properties investigated are the filtrate loss volume (API and HTHP FL) and cake thickness (API and HTHP FCT). These properties are shown in Fig. 12 (filtrate loss volume) and Fig. 13 (filter cake thickness). According to Fig. 12, a significant decrease in FL was observed with the inclusion of modified NC with increasing concentration in the BM at API and HTHP conditions. This is because a high specific area and small size of particles (exhibited by the modified NC) can provide a better sealing through a filter cake (Medhi et al., 2020). When 0.5 ppb PHPA was introduced, the API and HTHP FL values also became lower because bentonite particles – PHPA molecules can form a relatively thin filter cake to provide better sealing. This factor is often seen as an advantage for applying PHPA in a bentonite drilling mud system (Ercan and Ozbayoglu, 2009).

A higher filtrate loss volume implies a thicker filter cake. According to Fig. 13, the FCT of the BM was reduced with the NC with an increase in concentration. The optimum concentration of the modified NC in controlling filtration was found at 1.2 ppb. With 0.5 ppb, the API FCT of PHPA and modified NC muds decreased to 1.5 mm and 1.43 mm, respectively (Fig. 13). The same trend was observed in the HTHP FCT for the two products. These values are within the recommended API protocols and are not large to cause stuck pipe incidents in drilling operations. The inclusion of the modified NC in the BM minimized the filtration by controlling bentonite flocculation because a flocculated mud gives room for an easy flow of fluid into the formation (Al-Awad, 1998). Based on these results (rheological characterization and filtration

Table 3
Summary of Power-law model data for modified NC and 0.5 ppb PHPA mud systems before aging.

The operating temperature of 25 °C before thermal aging		
Concentration (ppb)	Flow behaviour index (n) (–)	Flow consistency index (K) (Pa)
WBM	0.406	158.44
0.4 ppb NC	0.389	216.82
0.5 ppb NC	0.368	252.30
0.8 ppb NC	0.358	284.97
1.2 ppb NC	0.322	363.57
0.5 ppb PHPA	0.477	258.31

Table 4
Summary of Power-law model data for modified NC and 0.5 ppb PHPA mud systems after aging for 16 h.

The operating temperature of 150 °C after thermal aging		
Concentration (ppb)	Flow behaviour index (n) (–)	Flow consistency index (K) (Pa)
WBM	0.438	100.45
0.4 ppb NC	0.437	150.68
0.5 ppb NC	0.406	184.85
0.8 ppb NC	0.394	214.54
1.2 ppb NC	0.372	251.11
0.5 ppb PHPA	0.472	212.65

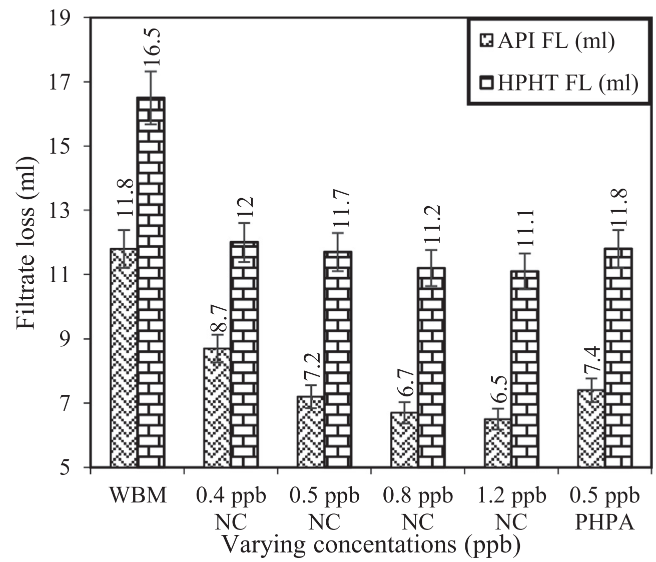

Fig. 12. API and HPHT filtrate loss of varying mud concentrations.

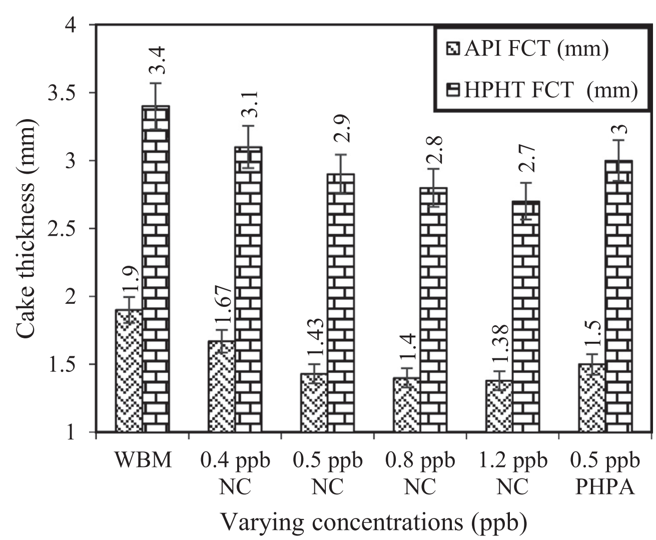

Fig. 13. API and HPHT filter cake thickness of varying mud concentrations.

properties), it can be concluded that PP-SiO_2 NC-NH_2 particles exhibited better characteristics in the WBM than the 0.5 ppb PHPA. At increasing concentration, they displayed a higher degree of temperature stability. If this character persists under the bottom-hole conditions of HTHP, it, then, implies that the modified NC can be more contributing to drilling operations.

4. Cuttings transport analysis

4.1. Influence of modified PP–SiO_2 NC on CTE

Fig. 14a–d present the CTE values of different cuttings types at a constant diameter range between 0.50 and 0.85 mm.

According to Fig. 14, the CTE values of the different cuttings types at a constant cuttings diameter in the range between 0.50 and 0.85 mm were compared using different annular velocities (66.1–138.6 ft/min) to comprehend the influence of the modified NC on the complex WBM system. A constant cuttings diameter of 0.50–0.85 mm was chosen from each of the sand grains because smaller sand particles tend to disperse in WBMs (Ozbayoglu and Sorgun, 2010). The plots of these figures showed that the CTE of the BM was increased by the inclusion of modified NC with increasing concentration. The impact was higher with increasing annular velocity. The ability of the modified NC to improve the lifting capacity of the complex WBM could be linked to the rather high average specific surface area (13.7 m^2/g) and narrow size distribution from 80 to 390 nm of the PP-SiO_2 NC-NH_2 particles, as reported in Fig. 6. These factors increased their interaction and distribution in the WBM, as shown in Fig. 15. It made the modified NC displayed a stronger Brownian motion in the mud, which caused the particles to collide more randomly and continuously (increased frequency of particle–particle interaction). This behaviour weakened the effect of gravity on the sand particles and led to higher cuttings transport capacity than the BM.

4.2. Influence of pipe rotation on CTE

Fig. 16 shows the results of CTE when a concentration of 0.5 ppb PHPA and modified NC concentrations were introduced into a BM with and without a pipe rotation speed of 150 rpm. This mud composition was investigated at different hole angles at a fixed flow rate of 42 L/min (0.042 m^3/min) using only sandstone of different sizes. Regarding the influence of the hole angle on CTE, the different plots shown in Fig. 16a-d demonstrate that the CTE values were decreased with increasing diameters of cuttings with or without pipe rotation at a constant flow rate of 42 L/min.

The highest cuttings recovered for each mud system occurred in the vertical annulus (0°) because of the drag force associated with the mud flow transformed into a lift force when acting in parallel with gravity (Oseh et al., 2019c). The next-highest recovery was achieved at the horizontal section (90°) of the well because the dominant force (axial drag force) was not affected by hole inclination, and hence, the cuttings did not avalanche during circulation (Bilgesu et al., 2007). The CTE at 30° inclinations was the third-highest, while the second-lowest occurred at 60°. The 45°-pipe angle experienced the lowest wellbore cleaning because the lift forces which dominate cuttings lifting decreased significantly (zero velocity on the low side of the hole) owing to the complex hole geometry (Bilgesu et al., 2007).

For the influence of pipe rotation on CTE, the shape of the trend lines of various sizes of the sandstone grains without pipe rotation is similar to those with pipe rotation but the performance of the mud samples was increased with pipe rotation for all cuttings sizes. The performance displayed by the muds improved more with pipe rotation due to the exposure of more cuttings to the top of the annulus having a higher circulation rate (Boyou et al., 2019). The CTE of 0.5 ppb NC is almost similar to that of 0.5 ppb PHPA sample but at higher diameters (2.00–2.40 mm) and (2.80–3.20 mm) of cuttings, the modified NC showed higher CTE than the PHPA.

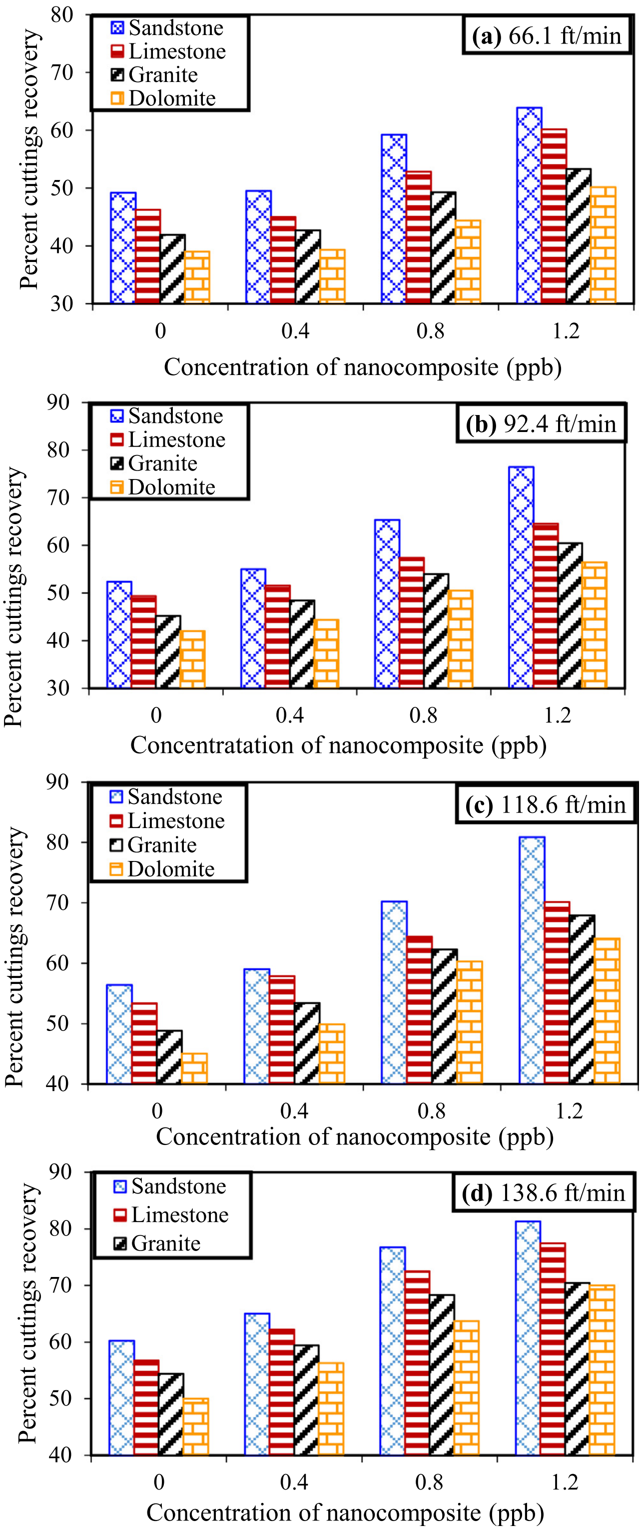

Fig. 14. CTE of varying mud systems at 60°-hole angle and sand diameter of range 0.50–0.85 mm.

The target of drilling is to produce crude oil while ensuring proper cuttings removal to the surface for disposal. If there exists a stationary bed, normally, an increase in the mud velocity will

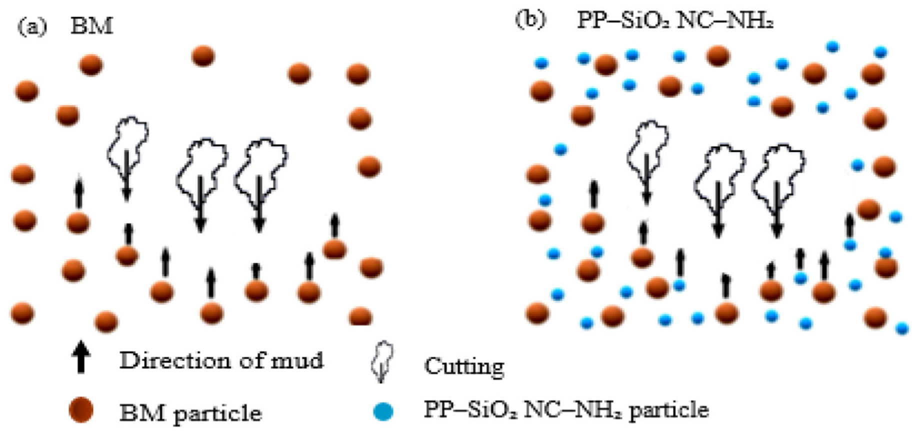

Fig. 15. Spreading of (a) BM particles and (b) modified NC particles in flowing mud streams.

erode the bed considerably. Nevertheless, subject to the drilling situations, a very large mud velocity is required to erode cuttings bed, which may not be implemented because of hydraulic and physical limitations (Fattah et al., 2011; Oseh et al., 2019c, 2019a). In such a condition, applying pipe rotation will be necessary to improve wellbore cleaning even with a mud velocity lower than the critical annular velocity. It can, therefore, be concluded that pipe rotation and enough flow rate should be considered when planning a cuttings transport program for enhanced wellbore cleaning.

5. Conclusions

In this study, the influence of annular velocities between 66 and 138.6 ft/min, 0.50–3.20 mm cuttings diameters, and a 60°-pipe angle on the CTE of modified NC mud systems were investigated. Also, a 0.5 ppb at a pump rate of 42 L/min (0.042 m^3/min) and different hole angles (0, 30, 45, 60, and 90°) were used to compare between the CTE of modified NC and PHPA with or without a pipe rotation speed of 150 rpm. The following conclusions were drawn based on the research goals and the results reached:

1. The ζ-potential data revealed the stability and the long-term stabilization of the modified NC in drilling muds. PSD data specifies that the modified product has a narrow size distribution from 80 to 390 nm. FESEM and TGA also confirmed the formation and modification of the NC.
2. Unlike the 0.5 ppb PHPA that decreased the shear-thinning character (n) of the WBM system, the modified NC increased the shear-thinning property of the mud system with increasing concentration at 25 and 150 °C. Further, a significantly viscous mud was observed using the 0.5 ppb PHPA compared to all the mud samples of the NC.
3. The CTE of 0.5 ppb modified NC + WBM was better than that of 0.5 ppb PHPA + WBM, especially at the worst hole angle of 45°. The poorest sand grains were transported at 45° followed by 60°, 30°, 90°, and 0°. In contrast with the smallest and intermediate sand grains, the lifting of the largest cuttings was complex and complicated.
4. Higher annular velocities and pipe rotation with 1.2 ppb (optimum concentration) of the NC showed more improvements in the cuttings lifting program and could be beneficial for enhanced cuttings transport process.

CRediT authorship contribution statement

Jeffrey O. Oseh: Conceptualization, Methodology, Validation, Formal analysis, Investigation, Data curation, Writing - original draft, Writing - review & editing. **M. N. A. M Norddin:** Conceptualization, Resources, Data curation, Supervision, Project administration, Funding acquisition. **Issham Ismail:** Validation, Supervision. **Augustine Agi:** Software, Validation. **Afeez O. Gbadamosi:** Software, Visualization. **Abdul R. Ismail:** Project administration. **Prasad Manoger:** Methodology, Formal analysis, Investigation, Data curation, Writing - original draft. **Kumaresan Ravichandran:** Methodology, Formal analysis, Investigation, Data curation, Writing - original draft.

Declaration of Competing Interest

The authors declare that they have no known competing financial interests or personal relationships that could have appeared to influence the work reported in this paper.

Acknowledgments

The authors wish to thank the Ministry of Higher Education Malaysia (MOHE) and Universiti Teknologi Malaysia Research Management Centre for funding this project under the Fundamental Research Grant Scheme (FRGS) with reference number FRGS/1/2019/TK05/UTM/02/20.

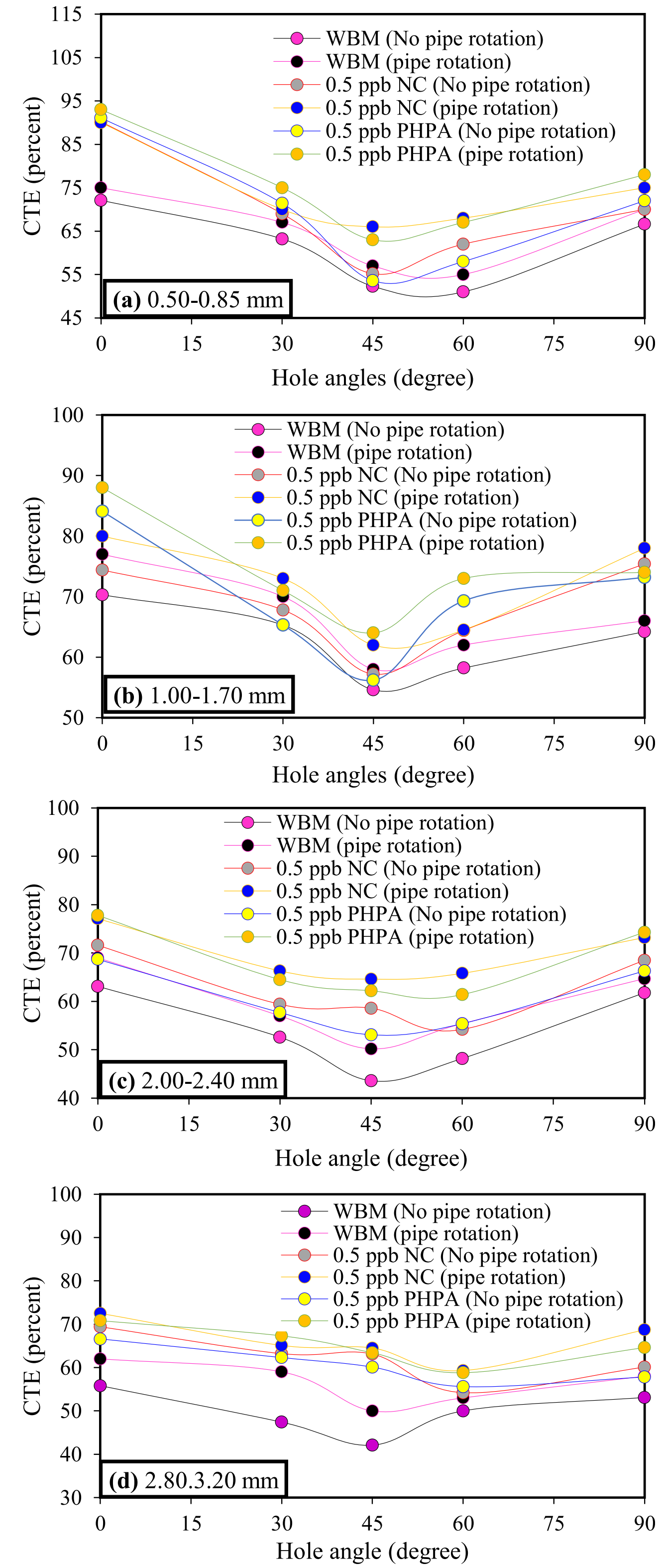

Fig. 16. Effect of pipe and non-pipe rotation on CTE of drilling muds at a flow rate of 42 L/min (0.042 m^3/min).

References

Al-Awad, M.N.J., 1998. Rheology and corrosivity of drilling fluids formulated from Al-Ghatt Saudi clays. J. King Saud Univ. – Eng. Sci. 10 (2), 285–298.

Al-Awad, M.N.J., 2001. Relationship between reservoir productivity and pore pressure drop. J. King Saud Univ. – Eng. Sci. 13 (1), 137–150.

Al-Awad, M.N.J., Al-Qasabi, A.O., 2001. Characterization and testing of Saudi Barite for potential use in drilling operations. J. King Saud Univ. – Eng. Sci. 13 (2), 287–298.

Al-Homadhi, E.S., 2009. Improving Local bentonite performance for drilling fluids applications. J. King Saud Univ. – Eng. Sci. 21 (1), 45–52.

API recommended practice 13B-1., 2017. API standard practice for field testing water-based drilling fluids, 5 ed(s). pp. 1–121.

ASTM D4253-00., 2006. Standard Test Methods for Maximum Index Density and Unit Weight of Soils Using a Vibratory Table. ASTM International, West Conshohocken, PA. https://doi.org/10.1520/D4253-00R06.

Bilgesu, H.I., Mishra, N., Ameri, S., 2007. Understanding the Effect of Drilling Parameters on Hole Cleaning in Horizontal and Deviated Wellbores Using Computational Fluid Dynamics. SPE-111208-MS. SPE Eastern Regional Meeting, 17–19 October, Lexington, Kentucky. pp. 1–7.

Boyou, N.V., Ismail, I., Sulaiman, W.R.W., Haddad, A.S., Hussein, N., Heah, T.H., Nadaraja, K., 2019. Experimental investigation of hole cleaning in directional drilling by using nano-enhanced water-based drilling fluids. J. Pet. Sci. Eng. 176, 220–231. https://doi.org/10.1016/j.petrol.2019.01.063.

Dahab, A.S., Al-Blehed, M.S., 1992. Testing of Saudi shales for potential use in drilling fluids. J. King Saud Univ. – Eng. Sci. 4 (21), 211–226.

Elkatatny, S., Kamal, M.S., Alakbari, F., Mahmoud, M., 2018. Optimizing the rheological properties of water-based drilling fluid using clays and nanoparticles for drilling horizontal and multi-lateral wells. Appl. Rheol. 28, 43606.

Elochukwu, H., Gholami, R., Dol, S.S., 2017. An approach to improve the cuttings carrying capacity of nanosilica based muds. J. Pet. Sci. Eng. 152, 309–316.

Ercan, C., Ozbayoglu, M.E., 2009. PHPA as a frictional pressure loss reducer and its pressure loss estimation. In: Middle East Drilling Technology Conference & Exhibition. doi:10.2118/125992.

Fattah, K.A., El-Katatney, A.M., Dahab, A.A., 2011. Potential implementation of underbalanced drilling technique in Egyptian oil fields. J. King Saud Univ. – Eng. Sci. 23 (1), 49–66.

Katende, A., Segar, B., Ismail, I., Sagala, F., Saadiah, H.H.A.R., Samsuri, A., 2020. The efect of drill–pipe rotation on improving hole cleaning using polypropylene beads in water based mud at diferent hole angles. J. Petrol. Explor. Prod. 10, 1253–1262.

Lam, C., Martin, P.J., Jefferis, S.A., 2015. Rheological properties of PHPA polymer support fluids. J. Mater. Civ. 27 (04015021).

Mao, H., Qiu, Z., Shen, Z., Huang, W., 2015. Hydrophobic associated polymer based silica nanoparticles composite with core–shell structure as a filtrate reducer for drilling fluid at ultra-high temperature. J. Pet. Sci. Eng. 129, 1–14.

Medhi, S., Chowdhury, S., Gupta, D.K., Mazumdar, A., 2020. An investigation on the effects of silica and copper oxide nanoparticles on rheological and fluid loss property of drilling fluids. J. Pet. Expl. Prod. Tech. 10, 91–100.

Nelson, E.B., Guillot, D., 2006. Well Cementing, Schlumberger 2nd ed. pp. 1-799. ISBN-13: 978-097885300-6

Oltedal, V.M., Werner, B., Lund, B., Saasen, A., Ytrehus, J.D. 2015. Rheological Properties of Oil Based Drilling Fluids and Base Oils. OMAE2015-41911, V010T11A042 Petroleum Technology, 10, 1–8.

Omurlu, C., Pham, H., Nguyen, Q.P., 2016. Interaction of surface-modified silica nanoparticles with clay minerals. Appl. Nanosci. 6 (8), 1167–1173.

Oseh, J.O., Mohd Norddin, M.N.A., Ismail, I., Gbadamosi, A.O., Agi, A., Ismail, A.R., 2020a. Experimental investigation of cuttings transportation in deviated and horizontal wellbores using polypropylene–nanosilica composite drilling mud. J. Pet. Sci. Eng. 106958, 1–24.

Oseh, J.O., Mohd Norddin M.N.A., Mohammed, H.N., Ismail, I., Gbadamosi, A.O., Agi, A., Ismail, A.R, Blkoor, S.O., 2020b. Influence of (3–Aminopropyl) triethoxysilane on entrapped polypropylene at nanosilica composite for shale swelling and hydration inhibition, J. Pet. Sci. Eng. 194.

Oseh, J.O., Mohd Norddin, M.N.A., Ismail, I., Ismail, A.R., Gbadamosi, A.O., Agi, A., 2019a. Effect of the surface charge of entrapped polypropylene at nanosilica-composite on cuttings transport capacity of water–based muds. Appl. Nanosci. 10 (1), 61–82.

Oseh, J.O., Mohd Norddin, M.N.A., Ismail, I., Ismail, A.R., Gbadamosi, A.O., Agi, A., Ogiriki, S.O., 2019b. Investigating almond seed oil as potential biodiesel-based drilling mud. J. Pet. Sci. Eng. 181 (106201), 1–16.

Oseh, J.O., Mohd Norddin, M.N.A., Ismail, I., Gbadamosi, A.O., Agi, A., Mohammed, H. N., 2019c. A novel approach to enhance rheological and filtration properties of water–based mud using polypropylene–silica nanocomposite. J. Pet. Sci. Eng. 181 (106264), 1–25.

Oseh, J.O., Norddin, M.N.A.M., Ismail, I., Gbadamosi, A.O., Agi, A., Ismail, A.R., Manoger, P., Ravichandran, K., 2020c. Enhanced cuttings transport efficiency of water-based muds using (3–Aminopropyl) triethoxysilane on polypropylene-nanosilica composite. Arabian J. Chem. https://doi.org/10.1016/j.arabjc.2020.07.004.

Ozbayoglu, M.E., Sorgun, F., 2010. Frictional Pressure Loss Estimation of Water-Based Drilling Fluids at Horizontal and Inclined Drilling With Pipe Rotation and Presence of Cuttings. In: SPE Oil and Gas India Conference and Exhibition, Mumbai, India.

Qiao, B., Wang, T.J., Ga, H., Jin, Y., 2015. High density silanization of nano-silica particles using γ-aminopropyltriethoxysilane (APTES). Appl. Surf. Sci. 351, 646–654.

Sayindla, S., Lund, B., Ytrehus, J.D., Saasen, A., 2017. Hole-cleaning performance comparison of oil-based and water-based drilling fluids. J. Pet. Sci. Eng. 159, 49–57.

Zu, L., Li, R., Jin, L., Lian, H., Liu, Y., Cui, X., 2013. Preparation and characterization of polypropylene/silica composite particle with interpenetrating network via hot emulsion sol-gel approach. Prog. Nat. Sci.: Mater. Int. 24, 42–49.